ISSN1027-5495. Functional Materials, 32, No.3 (2025), p. 498-507
doi:http://dx.doi.org/10.15407/fm32.03.498 © 2025 — STC "Institute for Single Crystals"

Synthesis, spectral properties and TD-DFT calculations of fluorescent mono and diphenyl substituted coumarin-3-carboxylic acids and their ethyl esters

P. V. Trostianko, A. V. Kyrychenko, O. N. Kalugin, S. M. Kovalenko

School of Chemistry, V. N. Karazin Kharkiv National University, 4 Svobody Sq., Kharkiv 61022, Ukraine.

Received March 22, 2025

In this study, efficient synthesis methods were developed for obtaining a systematic series of mono- and diphenyl-substituted coumarin-3-carboxylic acids and their ethyl esters. The UV absorption and fluorescence characteristics were determined in solvents of different polarity: nonpolar (cyclohexane) and polar aprotic (acetonitrile). The results showed that the position and number of phenyl substituents significantly affect the fluorescent properties of the obtained dyes. In addition, calculations based on the time-dependent density functional theory (TD-DFT) provided a detailed analysis of the electronic effects of phenyl substitution. Comparative spectral analysis and theoretical study of the structure-fluorescence relationship indicate that 7-phenyl-substituted coumarin-3-carboxylic acids among the studied derivatives are a promising platform for the development of innovative fluorescent materials, in particular for laser dyes, dye-sensitizers for solar cells, optoelectronics, and other fields.

Keywords: heterocyclic compounds, coumarin, organic dyes, dye-sensitized solar cell.

Синтез, спектральні властивості та TD-DFT розрахунки флуоресцентних моно та дифенілзаміщених 3-кумаринкарбонових кислот та їх етилових естерів. *П.В. Тростянко, О.В. Кириченко, О.М. Калугін, С.М. Коваленко*

Розроблено ефективні методики синтезу систематичного ряду моно- та дифенілзаміщених 3-кумаринкарбонових кислот і їх етилових естерів, визначено характеристики поглинання в УФ-діапазоні та флуоресценції у розчинниках різної полярності: неполярному (циклогексан) та полярному апротонному (ацетонітрил). Результати показали, що положення та кількість фенільних замісників суттєво впливають на флуоресцентні властивості отриманих барвників. Крім того, розрахунки на основі теорії часозалежного функціоналу густини (TD-DFT) забезпечили детальний аналіз електронних ефектів фенільного заміщення. Порівняльний спектральний аналіз і теоретичне вивчення взаємозв'язку структура–флуоресценція вказують на те, що 7-фенілзаміщені 3-кумаринкарбонові кислоти серед досліджених похідних становлять перспективну платформу для створення інноваційних флуоресцентних матеріалів, зокрема для лазерних барвників, барвників-сенсибілізоторів для сонячних комірок, оптоелектроніки та інших галузей.

1. Introduction

Coumarin dyes are known for their diverse spectral applications due to their adjustable photophysical properties, such as high quantum yields, solvatochromism, and sensitivity to environmental factors [1]. Specifically, 7-diethylamino-3-carboxy coumarin dyes exhibit variations in fluorescence intensity depending on the solvent or polymer matrix used. For instance,

higher quantum yields have been observed in chloroform and polyvinyl chloride, which is attributed to reduced intramolecular quenching in low-polarity environments [2]. These characteristics make coumarin dyes valuable for probing microenvironments in polymers and biological systems.

Coumarin derivatives, like Coumarin 120 (which is 7-amino-substituted), show enhanced fluorescence and reduced triplet-state losses (TSLs). These characteristics are essential for efficient laser operation [3, 4]. Additionally, coumarin-based dyes featuring D-π-A (donor-π bridge-acceptor) structures, including those that incorporate cyanoacetic acid or rhodanine acetic acid, are promising organic photosensitizers for dye-sensitized solar cells (DSSCs). They provide a broad absorption spectrum and facilitate efficient electron injection into TiO_2 [5].

Substituents at positions 3, 4 and 7 of the coumarin cores affect the optoelectronic properties. For instance, electron-donating groups, such as an amino group at position 7, result in red-shifted absorption and emission, expanding the potential for applications in dye lasers and solar cells [3].

The innovation and design of new coumarin dyes are driven by both scientific necessity and practical demands across various fields. A long-term strategy for development involves substitution engineering and extending the π-conjugation of the coumarin core [1, 3, 6]. In this study, we synthesized and characterized the spectral and fluorescence properties of a series of mono- and diphenyl-substituted coumarin-3-carboxylic acids and their esters. Our findings demonstrate that the position of phenyl group substitutions and the number of substitutions significantly affect the fluorescence properties of the new coumarin dyes. Additionally, we performed time-dependent density functional theory (TD-DFT) calculations to thoroughly analyze the electronic effects of phenyl substitution.

2. Experimental

Materials and Methods

Materials. The starting reagents were obtained from Sigma-Aldrich (USA) and were used without further purification. The reactions were monitored using thin-layer chromatography on Sorbfil UV-254 plates with a 1:2 (v/v) eluent mixture of ethyl acetate and hexane. Melting points were measured using a Cole-Parmer MP-250D standard digital melting point apparatus. Proton (^{1}H) NMR spectra were recorded on a Varian Gemini 400 MHz spectrometer, using deuterated dimethyl sulfoxide (DMSO-d_6) as the solvent. Liquid chromatography-mass spectrometry (LC/MS) was performed using a PE SCIEX API 150EX liquid chromatograph equipped with a UV detector set to λ_{max} 215 and 254 nm, along with a Luna-C18 column. The elution process started with water and ended with a mixture of acetonitrile and water (95:5, v/v) using a linear gradient at a flow rate of 0.15 mL/min over a total run time of 25 minutes.

DFT calculations. The structure of coumarin dye was first optimized using the density functional theory (DFT) approach with the B3LYP/cc-pVDZ method. To simulate a solution environment, the polarizable continuum model (PCM) for cyclohexane was applied. UV-visible absorption spectra were calculated using time-dependent DFT (TD-DFT) with the hybrid B3LYP functional [7] and the cc-pVDZ basis set [8]. All DFT calculations were performed using the Gaussian 16.C1 software package [9].

Synthesis

*General procedure for the synthesis of ethyl coumarin-3-carboxylates **(3a-f)***

Diethyl malonate **2** (160 mg, 1 mmol) was added to a solution of salicilyc aldehyde (1 mmol) in 10 ml of isopropanol. Then, piperidine (0.85 mg, 0.01 mmol) was added, and the reaction mixture was stirred at room temperature for 2 h. After the end of the reaction (TLC control), formed precipitate was filtered and washed with isopropanol and dried.

Ethyl coumarin-3-carboxylate (3a)

Yield: 210 mg (97%), white solid, mp = 94-95°C. ^{1}H NMR (400 MHz, DMSO-d_6) δ 8.76 (d, J = 0.7 Hz, 1H), 7.92 (dd, J = 7.7, 1.6 Hz, 1H), 7.74 (ddd, J = 8.4, 7.3, 1.7 Hz, 1H), 7.47 – 7.37 (m, 2H), 4.30 (q, J = 7.1 Hz, 2H), 1.31 (t, J = 7.1 Hz, 3H). LC/MS $[M+H]^+$ = 219.1.

Ethyl 5-phenylcoumarin-3-carboxylate (3b)

Yield: 274 mg (93%), white solid, mp = 131-132°C. ^{1}H NMR (400 MHz, DMSO-d_6) δ 8.81 (s, 1H), 7.93 (dd, J = 7.8, 1.6 Hz, 1H), 7.77 (dd, J = 7.6, 1.6 Hz, 1H), 7.65 – 7.58 (m, 2H), 7.56 – 7.41 (m, 4H), 4.31 (q, J = 7.6 Hz, 2H), 1.32 (t, J = 7.1 Hz, 3H). LC/MS $[M+H]^+$ = 295.2.

Ethyl 6-phenylcoumarin-3-carboxylate (3c)

Yield: 271 mg (92%), white solid, mp = 150-151°C. ^{1}H NMR (400 MHz, DMSO-d_6) δ 8.80 (s, 1H), 8.24 (d, J = 2.3 Hz, 1H), 8.03 (dd, J = 8.7,

2.3 Hz, 1H), 7.75 – 7.67 (m, 2H), 7.54 – 7.46 (m, 3H), 7.45 – 7.36 (m, 1H), 4.30 (q, J = 7.1 Hz, 2H), 1.32 (t, J = 7.1 Hz, 3H). LC/MS $[M+H]^+$ = 295.0.

Ethyl 7-phenylcoumarin-3-carboxylate (3d)

Yield: 277 mg (94%), white crystals, mp = 150-151°C. ^{1}H NMR (400 MHz, DMSO-d_6) δ 8.79 (s, 1H), 7.99 (d, J = 8.5 Hz, 1H), 7.83 (dd, J = 7.1, 1.8 Hz, 2H), 7.79 – 7.72 (m, 2H), 7.52 (dd, J = 8.3, 6.5 Hz, 2H), 7.49 – 7.42 (m, 1H), 4.31 (q, J = 7.1 Hz, 2H), 1.32 (t, J = 7.1 Hz, 3H). LC/MS $[M+H]^+$ = 295.0.

Ethyl 8-phenylcoumarin-3-carboxylate (3e)

Yield: 262 mg (89%), white solid, mp = 159-160°C. ^{1}H NMR (400 MHz, DMSO-d_6) δ 8.40 (s, 1H), 7.82 (ddd, J = 8.3, 7.5, 0.7 Hz, 1H), 7.62 – 7.54 (m, 2H), 7.54 – 7.50 (m, 1H), 7.50 – 7.44 (m, 3H), 7.40 (dt, J = 7.6, 0.9 Hz, 1H), 4.23 (qd, J = 7.1, 0.7 Hz, 2H), 1.23 (td, J = 7.1, 0.7 Hz, 3H). LC/MS $[M+H]^+$ = 295.0.

Ethyl 6,8-diphenylcoumarin-3-carboxylate (3f)

Yield: 307 mg (83%), yellow solid, mp = 197-199°C. ^{1}H NMR (400 MHz, DMSO-d_6) δ 8.86 (s, 1H), 8.27 (d, J = 2.3 Hz, 1H), 8.00 (d, J = 2.3 Hz, 1H), 7.83 – 7.76 (m, 2H), 7.75 – 7.68 (m, 2H), 7.58 – 7.45 (m, 5H), 7.45 – 7.37 (m, 1H), 4.32 (q, J = 7.1 Hz, 2H), 1.33 (t, J = 7.1 Hz, 3H). LC/MS $[M+H]^+$ = 371.0.

General procedure for the synthesis of coumarin-3-carboxylic acids (4a-f)

Solution of NaOH (30 mg, 0.75 mmol) in 5 ml of distilled H_2O was added to a suspension of **3a-f** (0.5 mmol) in 15 ml of iPrOH-H_2O 1:2 (v/v). The reaction mixture was refluxed for 2h, and then let to cool to room temperature. After the end of the reaction (TLC control), the reaction mixture was extracted with 3×10 ml $CHCl_3$. Aqueous phase was acidified with chilled 0.1 N HCl until a precipitate was formed. The precipitate was filtered and washed with 5 ml of iPrOH-H_2O 1:2 (v/v) and dried.

Coumarin-3-carboxylic acid (4a)

Yield: 89 mg (94%), white crystals, mp = 188-189°C. ^{1}H NMR (400 MHz, DMSO-d_6) δ 13.24 (s, 1H), 8.74 (s, 1H), 7.91 (dd, J = 7.7, 1.7 Hz, 1H), 7.73 (ddd, J = 8.7, 7.3, 1.6 Hz, 1H), 7.47 – 7.36 (m, 2H). LC/MS $[M+H]^+$ = 191.0.

5-Phenylcoumarin-3-carboxylic acid (4b)

Yield: 114 mg (86%), white solid, mp = 203-204°C. ^{1}H NMR (400 MHz, DMSO-d_6) δ 13.25 (s, 1H), 8.39 (d, J = 0.7 Hz, 1H), 7.80 (dd, J = 8.4, 7.6 Hz, 1H), 7.68 – 7.27 (m, 7H). LC/MS $[M+H]^+$ = 267.0.

6-Phenylcoumarin-3-carboxylic acid (4c)

Yield: 109 mg (82%), yellow crystals, mp = 218-220°C. ^{1}H NMR (400 MHz, DMSO-d_6) δ 13.29 (s, 1H), 8.80 (s, 1H), 8.24 (d, J = 2.3 Hz, 1H), 8.03 (dd, J = 8.7, 2.3 Hz, 1H), 7.72 (d, J = 7.4 Hz, 2H), 7.51 (t, J = 8.9 Hz, 3H), 7.41 (t, J = 7.4 Hz, 1H). LC/MS $[M+H]^+$ = 267.0.

7-Phenylcoumarin-3-carboxylic acid (4d)

Yield: 122 mg (92%), beige solid, mp = 249-251°C. ^{1}H NMR (400 MHz, DMSO-d_6) δ 13.19 (s, 1H), 8.78 (s, 1H), 7.98 (d, J = 8.5 Hz, 1H), 7.86 – 7.79 (m, 2H), 7.75 (td, J = 4.3, 1.8 Hz, 2H), 7.52 (dd, J = 8.3, 6.5 Hz, 2H), 7.49 – 7.42 (m, 1H). LC/MS $[M+H]^+$ = 267.0.

8-Phenylcoumarin-3-carboxylic acid (4e)

Yield: 108 mg (81%), white crystals, mp = 219-220°C. ^{1}H NMR (400 MHz, DMSO-d_6) δ 13.33 (s, 1H), 8.81 (s, 1H), 7.92 (dd, J = 7.8, 1.6 Hz, 1H), 7.76 (dd, J = 7.6, 1.6 Hz, 1H), 7.65 – 7.58 (m, 2H), 7.57 – 7.41 (m, 4H). LC/MS $[M+H]^+$ = 267.0.

6,8-Diphenylcoumarin-3-carboxylic acid (4f)

Yield: 110 mg (83%), yellow solid, mp = 214-215°C. ^{1}H NMR (400 MHz, DMSO-d_6) δ 8.85 (s, 1H), 8.25 (d, J = 2.3 Hz, 1H), 8.00 (d, J = 2.3 Hz, 1H), 7.84 – 7.77 (m, 2H), 7.76 – 7.69 (m, 2H), 7.59 – 7.50 (m, 4H), 7.50 – 7.38 (m, 3H). LC/MS $[M+H]^+$ = 343.0.

3. Results and discussion

Synthesis. In this study, we synthesized a series of mono- and diphenyl-substituted coumarin-3-carboxylic acids (compounds **4a-f**) and their corresponding esters (compounds **3a-f**). We then examined the spectral properties of their solutions in cyclohexane (ε_0 = 2.02) and acetonitrile (ε_0 = 36.64), comparing them with those of their unsubstituted analogues.

Coumarin-3-carboxylic acids **4a-f** were synthesized through the alkaline hydrolysis of ethyl esters **3a-f** (see Fig. 1). The ethyl coumarin-3-carboxylates were produced via the Knoevenagel condensation reaction, which involved the corresponding salicylic aldehydes **1a-f**. These aldehydes were initially obtained through the Suzuki-Miyaura cross-coupling reaction, in conjunction with diethyl malonate **2**, using a piperidine catalyst [10-12].

Some earlier works [13, 14] describe a one-step method for synthesizing coumarin-3-car-

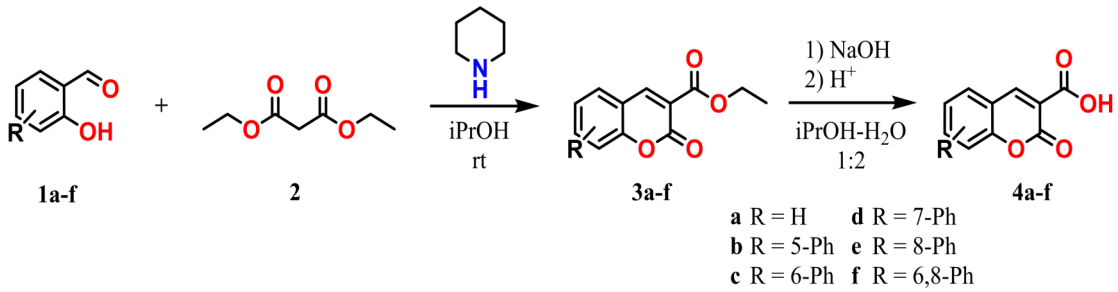

Figure 1. Scheme of synthesis of coumarin-3carboxylic acids **4a-f** and their esters **3a-f**

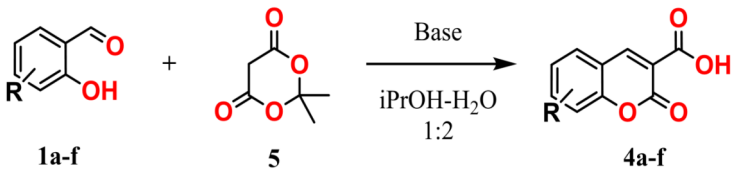

Figure 2. Scheme for the synthesis of coumarin-3-carboxylic acids **4a-f** by a one-reactor method

boxylic acids **4a-f** by condensing the corresponding salicylic aldehydes **1a-f** with Meldrum's acid (**5**) in the presence of a sodium azide and triethylamine catalyst (Fig. 2).

Table 1 presents the results of synthesized esters **3a-f** through the Knoevenagel reaction, as well as acids **4a-f** using three different methods. The one-reactor method is convenient and yields results consistent with previously published high yields for this reaction. However, there is incomplete conversion of the starting aldehyde due to its low solubility in the aqueous solvent mixture. As a result, the products obtained require additional purification by chromatographic methods to achieve spectral purity.

The two-step method produces pure products. In some rare cases, esters may need to be recrystallized from isopropanol, while acids can be effectively purified by extracting impurities with chloroform before the final product isolation. This simplified process for preparing pure

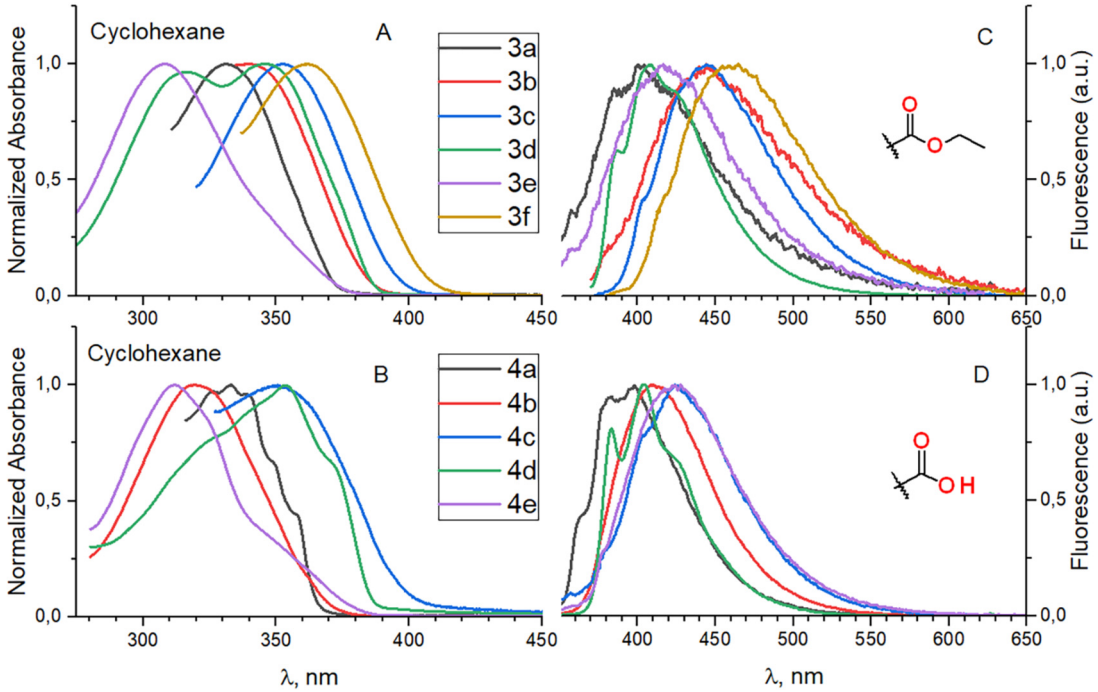

Fig. 3. Absorption and fluorescence spectra of coumarins **3a-f** (A, C) and **4a-e** (B, D) in cyclohexane

Table 1. Synthesis of coumarin-3-carboxylic acids **4a-f** and their esters **3a-f**.

Comp.	Catalyst (mol. %)	T, °C	time, h	yield , %
3a	Pyperidine (1% mol)	rt	2	97
3b	Pyperidine (1% mol)	rt	2	93
3c	Pyperidine (1% mol)	rt	2	92
3d	Pyperidine (1% mol)	rt	2	94
3e	Pyperidine (1% mol)	rt	2	89
3f	Pyperidine (1% mol)	rt	2	83
4a	NaOH (150 mol%)	reflux	2	94
	NaN_3 (50 mol%)	rt	20	81
	NEt_3 (30 mol%)	70	6	88
4b	NaOH (150 mol%)	reflux	2	86
	NaN_3 (50 mol%)	rt	20	90
	NEt_3 (30 mol%)	70	6	91
4c	NaOH (150 mol%)	reflux	2	82
	NaN_3 (50 mol%)	rt	20	84
	NEt_3 (30 mol%)	70	6	86
4d	NaOH (150 mol%)	reflux	2	92
	NaN_3 (50 mol%)	rt	20	89
	NEt_3 (30 mol%)	70	6	80
4e	NaOH (150 mol%)	reflux	2	81
	NaN_3 (50 mol%)	rt	20	86
	NEt_3 (30 mol%)	70	6	92
4f	NaOH (150 mol%)	reflux	2	83
	NaN_3 (50 mol%)	rt	20	60
	NEt_3 (30 mol%)	70	6	74

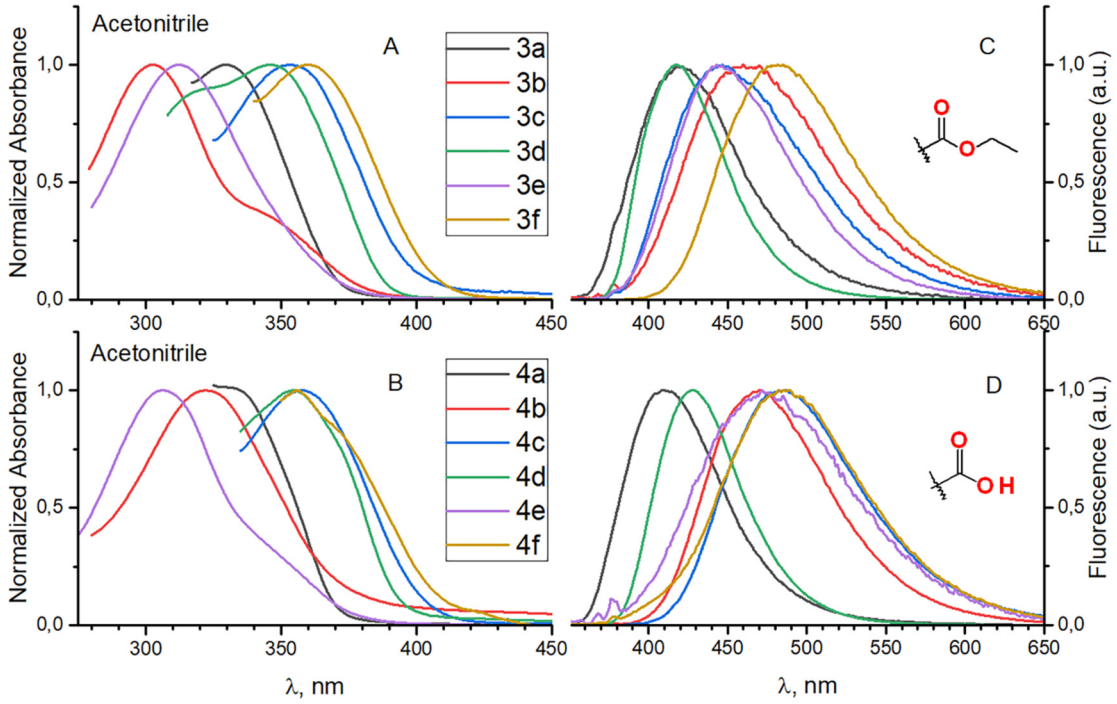

Fig. 4. Absorption and fluorescence spectra of coumarins **3a-f** (A, C) and **4a-f** (B, D) in acetonitrile

Table 2. Spectral properties of solutions of coumarin-3-carboxylic acids **4a-f** and their ethyl esters **3a-f** in cyclohexane and acetonitrile

Compounds	Cyclohexane			Acetonitrile		
	λ^{a}_{max}, nm	λ^{f}_{max}, nm	$\Delta\nu_{ST}$, cm^{-1}	λ^{a}_{max}, nm	λ^{f}_{max}, nm	$\Delta\nu_{ST}$, cm^{-1}
3a	331 287	400	5200	330 290	418	6400
3b	340 302	443	6850	351* 303	460	6750
3c	353 295	444	5800	354 294	447	5900
3d	346 316	408	4400	346 322	417	4900
3e	348* 308	417	4760	350* 312	443	6000
3f	362 304	464	6070	360 304	482	7000
4a	332 326	398	5000	335 299	408	5300
4b	351 319	409	4100	352 245	470	7100
4c	351 313	424	4900	358 301	486	7400
4d	354 323*	404	3500	355 317*	427	4800
4e	347** 312	427	5400	354* 306	472	7000
4f	—**	—	—	356 308	486	7500

* - estimated by the first derivative peak

** -compound 4f is almost insoluble in cyclohexane

compounds suitable for further spectral characterization is a significant advantage of the two-step method.

Spectral and Fluorescence Properties. UV-vis absorption and fluorescence spectra of coumarins **3a-f** and **4a-f** were measured in non-polar cyclohexane and aproton polar acetonitrile solvents (Figs. 3-4).

Table 2 presents the studied spectral properties, including the wavelengths of absorption (λ^{a}_{max}) and fluorescence (λ^{f}_{max}) maxima, and Stokes shift ($\Delta\nu_{ST}$) for the two solutions of compounds **3a-f** and **4a-f**.

First, we examine the photophysical properties of coumarins **3b-f** and **4b-e**, which are positional isomers that differ only in the location of the phenyl group on the coumarin scaffold (see Fig. 3). In cyclohexane solution, the absorption peaks of **4b-e** occur at 351, 354, and 347 nm, respectively. The corresponding emission peaks were measured at 409, 424, 404, and 427 nm. These results indicate that the first absorption band in the UV–vis absorption spectrum of all phenyl-substituted coumarins is positioned at longer wavelengths compared to the unsubstituted coumarin **4a**, although with varying degrees of redshift (see Fig. 3C). The similar trends were observed in fluorescence spectra, as illustrated in Fig. 3D. The largest Stokes shifts of 4900 and 5400 cm^{-1}, along with redshifted emissions, were observed for coumarins **4c** and **4e**, which have the phenyl substituent located at positions 6 and 8, respectively.

In polar acetonitrile, both absorption and fluorescence bands of coumarins **4a-f** and their ethyl esters **3a-f** revealed red spectral shifts, as illustrated in Fig. 4 and Table 2.

DFT and TD-DFT Calculations. TD-DFT calculations have become convenient tool for

Table 3. The first three excited-state vertical electronic transitions $S_0 \rightarrow S_n$ (where n=1-3), their oscillator strength f, and electronic configuration calculated at the TD-B3LYP/cc-pVDZ(PCM=cyclohexane) level.

Compounds	λ^a_{max}, nm	Oscillator strength, f	Comparison with Experiment, nm[a]	Electronic Configurations
3a	331.3 291.7 251.7	0.2151 0.3301 0.0003	0.3	H-L 0.67566 H-1-L 0.66489 H-L+1 0.66067 H-L 0.18547
3b	346.5 326.2 302.5	0.0826 0.4033 0.0008	6.5	H-L 0.69605 H-1-L 0.68949 H-3-L 0.59769 H-4-L -0.24031
3c	369.5 298.4 297.7	0.1124 0.0001 0.4560	16.5	H-L 0.69720 H-2-L -0.16528 H-4-L 0.67690 H-1-L 0.67596 H-2-L -0.12353
3d	355.5 321.2 300.8	0.8034 0.0926 0.0020	9.5	H-L 0.69489 H-1-L 0.68387 H-3-L 0.18272 H-4-L 0.66590
3e	363.7 318.0 309.5	0.0594 0.4082 0.0022	19.3	H-L 0.69651 H-1-L 0.68859 H-3-L 0.69028 H-2-L -0.13591
3f	383.7 332.9 309.9	0.0791 0.1948 0.0004	21.7	H-L 0.69816 H-1-L 0.69275 H-3-L 0.69180 H-5-L 0.13271
4a	333.9 293.2 290.6	0.1824 0.3068 0.0001	0.9	H-L 0.69246 H-1-L 0.66187 H-L 0.18763 H-3-L 0.66827 H-2-L -0.19406
4b	373.7 341.8 333.7	0.0745 0.3009 0.0244	22.7	H-L 0.70003 H-1-L 0.67561 H-3-L 0.14773 H-2-L -0.25922 H-4-L 0.62577
4c	374.3 301.2 298.8	0.0956 0.0091 0.4278	23.3	H-L 0.69777 H-2-L 0.67237 H-1-L 0.20558 H-2-L -0.19902 H-1-L 0.65694
4d	358.0 324.5 301.2	0.7461 0.0844 0.0062	4.0	H-L 0.69455 H-1-L 0.66797 H-2-L 0.69146
4e	369.5 320.0 314.6	0.0528 0.3573 0.0043	22.5	H-L 0.69726 H-1-L 0.68681 **H-2-L 0.69756**
4f	389.4 337.8 315.2	0.0689 0.1606 0.0004	-	H-L 0.69885 H-1-L 0.69345 H-2-L 0.70058

a – the comparison with the experimental spectra measured in cyclohexane was calculated as $\lambda^a_{max(TD\text{-}DFT)}$- $\lambda^a_{max(experimental)}$, where $\lambda^a_{max(experimental)}$ corresponds to the maximum of the most long-wave length absorption band.

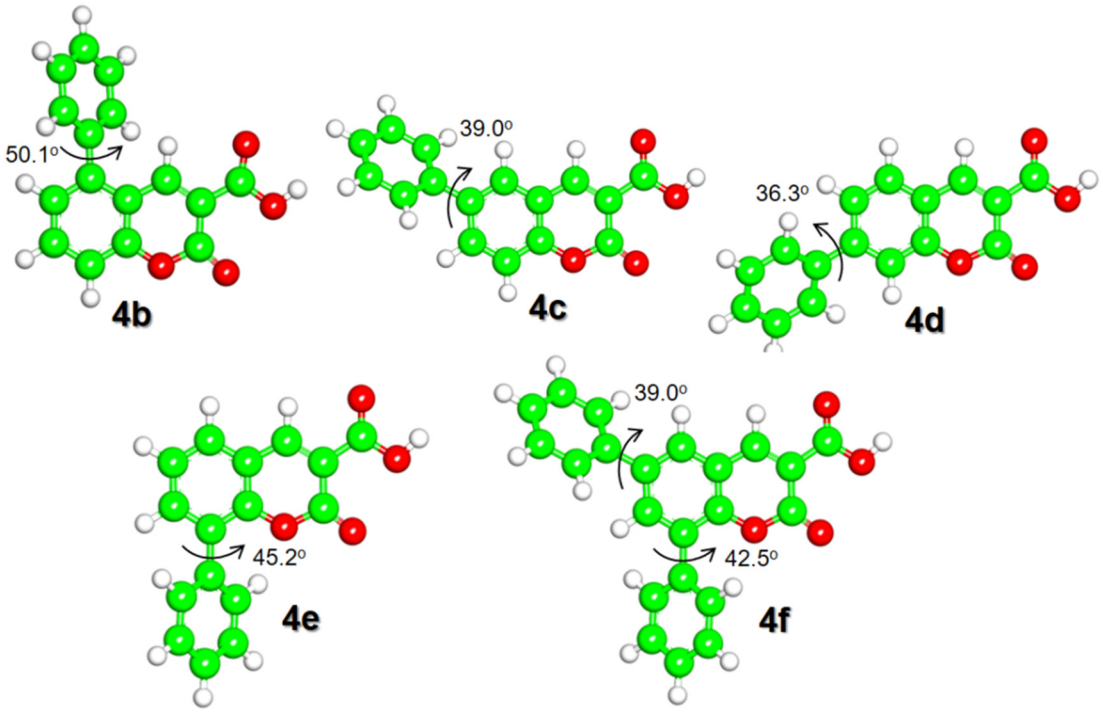

Fig. 5. The ground-state geometry of coumarins **4b-f** optimized by the B3LYP/cc-pVDZ(PCM=cyclohexane) method

studying electronic structure and spectra of coumarins and other dyes [1, 15-18].

To better understand the molecular origin of the various photophysical properties of phenyl-substituted coumarins, we performed DFT and TD-DFT calculations. We optimized the ground-state geometry of the studied coumarins at the B3LYP/cc-pVDZ (PCM=cyclohexane) level of theory. Our findings indicate that, for all studied derivatives, the phenyl moiety π-conjugated with the coumarin chromophore does not adopt an overall planar structure. Instead, the phenyl group is twisted at an angle ranging from 36 to 50 degrees depending on substitution position, as summarized in Figure 5.

The vertical excited-state transitions $S_0 \rightarrow S_n$ were calculated for the ten lowest singlet excited states at the TD-B3LYP/cc-pVDZ(PCM=cyclohexane) level. The excited-state characteristics and electronic configurations for three lowest transitions are summarized in Table 3.

The TD-DFT simulated UV-vis absorption properties indicate that the substitution of the coumarin with one or two phenyls, which have an electron-donating character, results in a red shift in the long-wavelength band. The calculated absorption spectra of coumarins **4a-f** were in good agreement with the experiment (see Table 3 and Fig. 3).

The TD-DFT data can be rationalized by the molecular orbital (MO) calculations shown in Figure 6 for the HOMO and LUMO, and other frontier orbitals. The analysis of electronic transitions and their orbital configurations (see Table 3) revealed that upon excitation, phenyl- and diphenyl-substituted coumarins undergo structural and electronic reorganization resulting in a redistribution of electron density from the phenyl ring to the coumarin chromophore. For all studied coumarins, the lowest vertical transition $S_0 \rightarrow S_1$ is characterized by the single configuration transition HOMO-LUMO and the high oscillator strength. In cases **4c**, **4e** and **4f,** this HOMO-LUMO transition has some charge-transfer (CT) character, as evidenced by the almost complete redistribution of electron density from the phenyl groups to the coumarin moiety.

4. Summary and Perspectives

Phenyl-substituted coumarins serve as an example of how structural modification can reveal their functional capabilities, such as spectral, electronic and material properties. The phenyl group extends π-conjugation, which can lead to enhanced fluorescence properties.

In this study, we designed and synthesized a series of mono- and diphenyl-substituted cou-

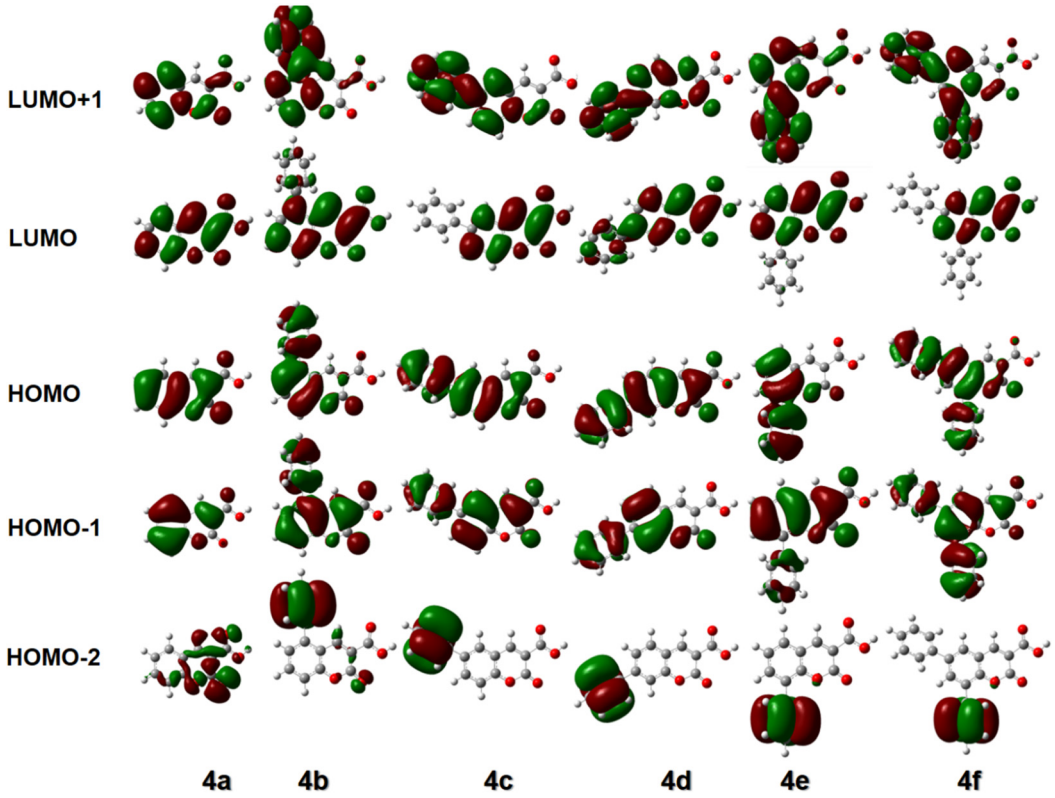

Fig. 6. Frontier molecular orbitals of compounds **4a-f** calculated by the TD-B3LYP/cc-pVDZ(PCM=cyclohexane) method.

marin-3-carboxylic acids and their esters. The UV-vis absorption and fluorescence characteristics were measured in solvents, such as non-polar cyclohexane and polar aprotic acetonitrile. The spectroscopic results demonstrated that the position and number of phenyl group substitutions significantly affect fluorescence properties of the obtained dyes. Our data suggested that the introduction of the phenyl moiety to C7-position of coumarin heterocycle resulted in largest bathochromic shifts in both absorption and fluorescence spectra, so that their Stokes shifts extend to 5500 cm^{-1} (Figs. 3-4 and Table 2). Additionally, we performed time-dependent density functional theory (TD-DFT) calculations to analyze the electronic effects of phenyl substitution in detail. Our spectral analysis combined with theoretical evaluation of the structure-fluorescence relationship suggests that 7-phenyl-substituted coumarin-3-carboxylic acid is a promising scaffold for developing a new fluorescent dyes.

Current trends in this field indicate that the most effective approach for the rational design of new coumarin dyes involves a combination of computational modeling, targeted structural modifications, and sustainable synthesis. Therefore, we believe that by using modern computational tools such as TD-DFT, next-generation coumarins have the potential to make breakthroughs in optoelectronics, biomedicine and other fields by addressing specific application needs.

Acknowledgments: The work was supported by Grant № 0121U112886 of the Ministry of Education and Science of Ukraine.

References

1. X. Liu, Z. Xu, J.M. Cole. *J. Phys. Chem. C*, **117** (32), 16584-16595 (2013).
2. M. Danko, E. Szabo, P. Hrdlovic. *Dyes and Pigments*, **90** (2), 129-138 (2011).
3. X. Liu, J.M. Cole, P.G. Waddell, T.-C. Lin, J. Radia, A. Zeidler. *J. Phys. Chem. A*, **116** (1), 727-737 (2012).
4. Y.O. Shaydyuk, N.V. Bashmakova, G.V. Klishevich, A.M. Dmytruk, O.D. Kachkovsky, I.B. Kuziv, I.Y. Dubey, K.D. Belfield, M.V. Bondar. *ACS Omega*, **8** (12), 11564-11573 (2023).
5. L. Han, H. Wu, Y. Cui, X. Zu, Q. Ye, J. Gao. *J. Photochem. Photobiol. A.*, **290**, 54-62 (2014).
6. A. Cocco, P. Caria, G. Sanna, L. Stagi, E. Cadoni, R. Corpino, P.C. Ricci, C.M. Carbonaro, F. Secci. *ACS Omega*, **6** (49), 33708-33716 (2021).
7. T. Yanai, D.P. Tew, N.C. Handy. *Chem. Phys. Lett.*, **393** (1), 51-57 (2004).

8. T.H. Dunning. *J. Chem. Phys.*, **90** (2), 1007-1023 (1989).
9. M.J. Frisch, G.W. Trucks, H.B. Schlegel, G.E. Scuseria, *et al*, in, Wallingford, CT, 2016.
10. B.T. Watson, G.E. Christiansen. *Tetrahedron Lett.*, **39** (33), 6087-6090 (1998).
11. S. Gurrapu, S.K. Jonnalagadda, M.A. Alam, C.T. Ronayne, G.L. Nelson, L.N. Solano, E.A. Lueth, L.R. Drewes, V.R. Mereddy. *Bioorg. Med. Chem. Lett.*, **26** (14), 3282-3286 (2016).
12. H. Ji, Y. Tan, N. Gan, J. Zhang, S. Li, X. Zheng, Z. Wang, W. Yi. *Bioorg. Med. Chem.*, **29**, 115870 (2021).
13. G. Brahmachari. *ACS Sustainable Chem. Eng.*, **3** (9), 2350-2358 (2015).
14. W.-Y. Pan, Y.-M. Xiao, H.-Q. Xiong, C.-W. Lü. *Res. Chem. Interm.*, **42** (9), 7057-7063 (2016).
15. R.G. Shypov, O.V. Buravov, E.S. Gladkov, L.V. Chepeleva, A.V. Kyrychenko. *Funct. Mater.*, **31** (3), 405-412 (2024).
16. M.M. Blazhynska, D.S. Stepaniuk, V. Koverga, A. Kyrychenko, A. Idrissi, O.N. Kalugin. *J. Mol. Liq.*, **332**, 115811 (2021).
17. D.S. Stepaniuk, M.M. Blazhynska, V. Koverga, A. Kyrychenko, F.-A. Miannay, A. Idrissi, O.N. Kalugin. *Mol. Simul.*, **48** (2), 99-107 (2022).
18. M.S.A. Abdel-Mottaleb. *Turk. J. Chem.*, **47** (1), 164-170 (2023).